

D-AXIS EQUIVALENT CIRCUIT MODELLING FROM TRANSIENT TESTS IN SYNCHRONOUS MACHINES

EDSON C. BORTONI*, JOSÉ V. BERNARDES JR*, PAULO V.V. SILVA*, VICTOR A.D. FARIA*

**Electrical and Energy Systems Institute, Federal University of Itajubá*

Av. BPS, 1303, Itajubá-MG, Brazil

E-mails: bortoni@unifei.edu.br, jusevitor@unifei.edu.br,

pvictor_vs@hotmail.com, duraes_victor@unifei.edu.br

Abstract— This paper revisits voltage recovery, sudden short-circuit, and load-rejection tests aiming at d-axis modelling of synchronous machines. Discussions are developed based on the calculus of equivalent circuit parameters from tests; in this discussions, the article also include methods to obtain the Canay reactance. Simulations and tests application in field and in laboratory are also presented.

Keywords—Canay Reactance, Load-Rejection Test, Parameter Identification, Sudden Short-Circuit Test, Synchronous Machines, Voltage Recovery Test.

Resumo— Esse trabalho revisita os ensaios de recuperação de tensão, curto circuito repentino e rejeição de carga objetivando a modelagem do eixo direto de máquinas síncronas. Discussões são desenvolvidas com base nos cálculos dos parâmetros do circuito equivalente a partir de ensaios; nessas discussões é incluindo métodos para a obtenção da reatância de Canay. Simulações e ensaios feitos em campo e em laboratório são apresentados ao final do artigo.

Palavras-chave— Ensaio de Rejeição de Carga, Ensaio de Curto-Circuito Repentino, Ensaio de Recuperação de Tensão, Identificação de Parâmetros, Máquinas Síncronas, Reatância de Canay.

Nomenclature

A, B, C	Auxiliary variables
i	Instantaneous armature current (p.u)
I	Armature effective current (p.u)
I_0	Long term armature effective current (p.u)
I_{fu}	Unidirectional field current (p.u)
r_f	Field winding resistance (p.u)
r_{1d}	Damper winding resistance (p.u)
I_{fu0}	Initial unidirectional field current (p.u)
T'_{d0}	Open-circuit d-axis transient time constant (s)
T''_{d0}	Open-circuit d-axis subtransient time constant (s)
T'_d	Short-circuit d-axis transient time constant (s)
T''_d	Short-circuit d-axis subtransient time constant (s)
T_{1d}	Damper winding time constant (s)
v	Instantaneous armature phase voltage (p.u)
V	Armature effective voltage (p.u)
V_0	Long term armature effective voltage (p.u)
X_d	D-axis synchronous reactance (p.u)
X'_d	D-axis transient reactance (p.u)
X''_d	D-axis subtransient reactance (p.u)
r_f	Field winding resistance (p.u)
r_{1d}	Damper winding resistance (p.u)
x_c	Canay reactance (p.u)
x_l	Armature leakage reactance (p.u)
x_{ad}	Armature mutual reactance (p.u)
x_f	Field winding leakage reactance (p.u)
x_{1d}	Damper winding leakage reactance (p.u)
x_{f1d}	Mutual damper to field leakage reactance (p.u)
ΔI_{fu0}	Initial variation of the field current (p.u)

1 Introduction

The three most applied transient tests for d-axis equivalent circuit modeling of synchronous machines are the sudden short-circuit, voltage-recovery, and load-rejection tests. The short-circuit test has been applied worldwide and it is recommended in the main standards for machine testing (IEEE, 2009; IEC, 2008; IEEE, 2014). Peak detection, interpolation, extrapolation, are some of the employed techniques to the analysis of the short-circuit current (Kamwa et al., 1995a, 1995b).

The voltage recovery test is also described in the main standards, but few of its applications have been reported in the technical literature (Bortoni, 2017; Martin and Tindall, 2000; Beordo, 2016), even though the setup arrangement is the same of the sudden short-circuit. The load-rejection test has been proposed by many authors (Melo and Ribeiro, 1977; Bortoni and Jardini, 2002; Wamkeue et al., 2011) and is readily applicable.

In order to avoid terminal overvoltage, the machine is usually under excited and demanding considerable reactive power. In fact, the voltage recovery test is similar to the d-axis load rejection test. Neglecting resistances, the short is a pure inductive load at null terminal voltage. When opening the short, the terminal voltage will increase to the open circuit voltage, which is the internal induced voltage for that applied field current.

The obtained parameters can be saturated or not. For power system non-connected tests, i.e., short-circuit and voltage recovery tests, saturated or non-

saturated parameters depend on the applied excitation current. If the excitation current is in the linear stretch of the no-load saturation curve, the obtained parameters are non-saturated, and if the excitation current is in the nonlinear stretch of the no-load saturation curve, the obtained parameters are saturated.

Since the armature current during the short-circuit test must be controlled, as so as the terminal voltage in the voltage-recovery test, these tests are in general made with a reduced field current and this way in the linear stretch of the no-load saturation curve.

The parameters obtained in the load-rejection are in general saturated, since initially, the machine is connected to a power system and the rated voltage is in the non-linear stretch of the no-load saturation curve. The obtained parameters can be non-saturated ones if a single load, e.g. a capacitance, is rejected from the synchronous generator.

On the other hand, the d-axis of a synchronous machine can be better modeled if damper to field windings mutual leakage reactance is taken into account, instead of considering its value equal to the other mutual reactances. All tests previously mentioned give the necessary information to calculate this reactance if the transient excitation current is recorded. It must be kept in mind that, in all the cases, the excitation voltage must be held constant during the tests.

The following sections revisit the d-axis modeling of a salient pole synchronous machine, including the effects of unequal mutual reactances. Simulations, field tests information and laboratory tests measurements are used to estimate the d-axis equivalent circuit parameters.

2 D-Axis Modeling

Figure 1a describes d-axis equivalent circuit of a synchronous machine with only one damper winding where the per unit value of all mutual inductances are considered as the same. Equations (1)-(5) can be used to obtain the p.u parameters of this equivalent circuit from the known p.u values X_d , X'_d , X''_d and x (IEEE, 2002).

For the circuit of Fig. 1a, the reactance x takes the value of the leakage reactance, x_l . Nevertheless, it is interesting to notice that it does not matter which value x assumes (including negative values), resulting in different circuit parameters values, the traditional parameters, X_d , X'_d , X''_d , will always be retrieved.

$$x_{ad} = X_d - x \quad (1)$$

$$x_f = \frac{(X_d - x)(X'_d - x)}{(X_d - X'_d)} \quad (2)$$

$$x_{1d} = \frac{(X'_d - x)(X''_d - x)}{(X'_d - X''_d)} \quad (3)$$

$$r_f = \frac{1}{\omega T'_d} \frac{X'_d (X_d - x)^2}{X_d (X_d - X'_d)} \quad (4)$$

$$r_{1d} = \frac{1}{\omega T''_d} \frac{X''_d (X'_d - x)^2}{X'_d (X'_d - X''_d)} \quad (5)$$

$$X_d = x + x_{ad} \quad (6)$$

$$X'_d = x + \frac{1}{\frac{1}{x_{ad}} + \frac{1}{x_f}} \quad (7)$$

$$X''_d = x + \frac{1}{\frac{1}{x_{ad}} + \frac{1}{x_f} + \frac{1}{x_{1d}}} \quad (8)$$

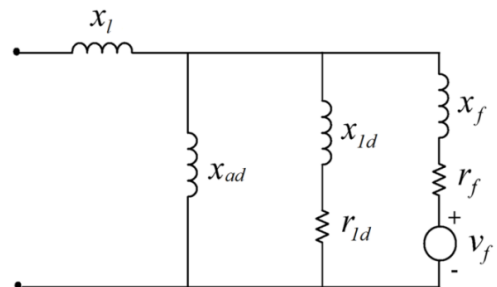
That is why this traditional circuit (Fig. 1a) works pretty well for armature quantities simulation; after all, it is constructed to match the traditional parameters (which were obtained from armature signals). On the other hand, it has been known for a long time that this circuit does not result in accurate field quantities calculations and simulations (Canay, 1969). As has been already shown, there are not enough degrees of freedom to make equal several mutual inductance values (Kamwa and Viarouge, 1994; Kirtley, 1994). Considering a given value for the leakage reactance, if one wants to make the p.u mutual reactance between field and damper windings equal to the other mutual reactances, eventually there will be a difference between the measured and simulated field quantities.

Instead, if the fidelity of rotor quantities simulation, such as torque and current, is desired, this mutual reactance (x_{f1d}) must eventually be unequal to the others, resulting in the circuit of Fig. 1b.

While considering the mutual reactance x_{f1d} , a transformation can be applied to the circuit of Fig. 1b to reach the form of the circuit of the Fig. 1(a), resulting in the circuit of Fig. 1c. In this case, a convenient value of x_c strongly related to x_{f1d} is used in place of x in equations (1)-(5), reaching modified parameters (using the subscript c). This relationship is given by (9).

$$\frac{1}{x_{f1d}} = \frac{1}{x_c - x_l} - \frac{1}{X_d - x_l} \quad (9)$$

With those values in hands, simulation tools designed to be used with the traditional circuit of Fig. 1a can still be employed, achieving fidelity of both armature and field windings. The challenge is to determine either x_c or x_{f1d} , that can be obtained by transient tests of voltage-recovery, load-rejection, and three-phase sudden short-circuit.



(a)

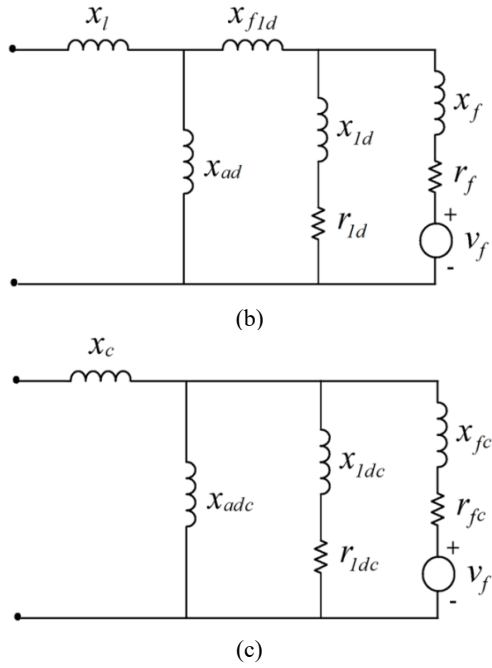


Figure 1. Direct axis equivalent circuits.

3 Analysis of Transient Tests

Sudden short-circuit, load-rejection and voltage recovery tests are well described in the main machine testing standards. The aim of the following sections is at revisiting such methods presenting analysis and equations to estimate x_c .

3.1 Voltage-recovery test

The voltage recovery test is applied to the short-circuited machine operating as a generator, driven at rated speed. Excitation winding is fed with a constant voltage to obtain a desired armature current, normally limited to its rated value. Suddenly the three-phase terminals of the machine are simultaneously opened, and both armature three-phase voltages and field current are recorded along the transient process. In this test, the terminal voltage steps from zero to a given value, and gradually grows until reaching its steady-state value.

The terminal voltage behavior in the voltage recovery test is depicted in Fig. 2a, and the equation that governs the RMS value of the terminal voltage is presented in (10).

$$V = I_0 \left[X_d - (X_d - X'_d) e^{-\frac{t}{T'_{d0}}} - (X'_d - X''_d) e^{-\frac{t}{T''_{d0}}} \right] \quad (10)$$

Taking into account the absolute values of A_1 , A_2 , and A_3 , depicted in Fig. 2a, the synchronous, transient and subtransient reactances are obtained from (11) to (13).

$$X_d = \frac{A_1}{I_0} \quad (11)$$

$$X'_d = \frac{A_2}{I_0} \quad (12)$$

$$X''_d = \frac{A_3}{I_0} \quad (13)$$

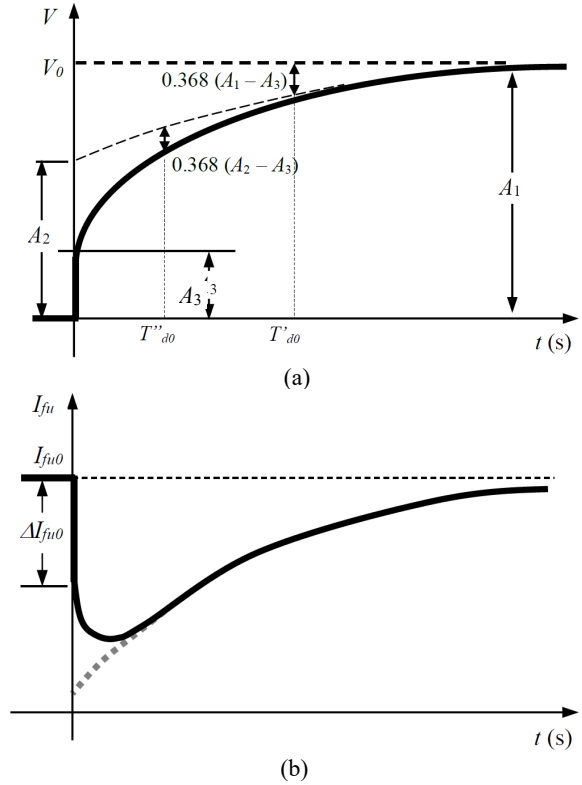


Figure 2. Quantities variation in the voltage-recovery test.

While the reactances and the time constants can be obtained geometrically, they can also be calculated mathematically through exponential linear regressions over the transient and subtransient periods.

Equation (14) describes the behavior of the unidirectional field current related to the initial field current, during the voltage recovery test, as depicted in Fig. 2b.

$$\frac{I_{fu}}{I_{fu0}} = 1 - \left(\frac{X_d - X'_d}{X_d} \right) \left[e^{-\frac{t}{T'_{d0}}} - \left(1 - \frac{T_{1d}}{T''_{d0}} \right) e^{-\frac{t}{T''_{d0}}} \right] \quad (14)$$

Equation (15) is obtained evaluating (14) in t equals to zero. Equation (16) comes from the equivalent circuit. Equation (17) results from (16) substituting making x equal to x_c .

$$\frac{T_{1d}}{T''_{d0}} = \frac{X_d}{X_d - X'_d} \frac{\Delta I_{fu0}}{I_{fu0}} \quad (15)$$

$$\frac{T_{1d}}{T''_{d0}} = \frac{X''_d - x}{X'_d - x} \quad (16)$$

$$x_c = \left(\frac{T_{1d}}{T''_{d0}} X'_d - X''_d \right) / \left(\frac{T_{1d}}{T''_{d0}} - 1 \right) \quad (17)$$

3.2 Sudden Short-Circuit Test

The sudden short-circuit test is applied to the open-circuited machine operating as a generator, driven at rated speed. Excitation winding is fed with a constant voltage to obtain unsaturated or saturated parameters. Then, the three-phase terminals of the machine are suddenly and simultaneously shorted. The resulting field and armature currents in all phases are recorded.

The RMS value of the armature current during the transient regime can be obtained by subtracting the superior envelope by the inferior envelope of the armature current and then dividing the result by the square root of two. Envelopes are determined from the current sinusoid peaks detection, interpolation, and extrapolation (IEEE, 2009)

The RMS value of the armature current behavior in the three-phase sudden short-circuit test is depicted in Fig. 3a, equation (18) model this phenomenon.

$$I = V_0 \left[\frac{1}{X_d} + \left(\frac{1}{X'_d} - \frac{1}{X_d} \right) e^{-\frac{t}{T'_d}} + \left(\frac{1}{X''_d} - \frac{1}{X'_d} \right) e^{-\frac{t}{T''_d}} \right] \quad (18)$$

Considering the absolute values of B_1 , B_2 and B_3 depicted in Fig. 3a, the synchronous, transient and subtransient reactances are obtained from (19) to (21).

$$X_d = \frac{V_0}{B_1} \quad (19)$$

$$X'_d = \frac{V_0}{B_2} \quad (20)$$

$$X''_d = \frac{V_0}{B_3} \quad (21)$$

The interaction with the unidirectional component of the armature short-circuit current will result in a first order sinusoid over the unidirectional component of the field current. The unidirectional component can be determined as the average of the superior and inferior field current envelopes.

The behavior of the unidirectional field current in face of short-circuit is described by (22) and is depicted in Fig. 3b.

$$\frac{I_{fu}}{I_{fu0}} = 1 + \left(\frac{X_d - X'_d}{X'_d} \right) \left[e^{-\frac{t}{T'_d}} - \left(1 - \frac{T_{1d}}{T''_d} \right) e^{-\frac{t}{T''_d}} \right] \quad (22)$$

Evaluating (22) in t equals to zero, (23) can be obtained. Equation (24) comes from the equivalent circuit, and (25) is the solution of (23) and (24) for x equal to x_c .

$$\frac{T_{1d}}{T''_d} = \frac{X'_d}{X_d - X'_d} \frac{\Delta I_{fu0}}{I_{fu0}} \quad (23)$$

$$\frac{T_{1d}}{T''_d} = \frac{X''_d - x}{X'_d - x} \frac{X'_d}{X''_d} \quad (24)$$

$$x_c = \left(\frac{T_{1d} X''_d}{T''_d X'_d} X'_d - X''_d \right) / \left(\frac{T_{1d} X''_d}{T''_d X'_d} - 1 \right) \quad (25)$$

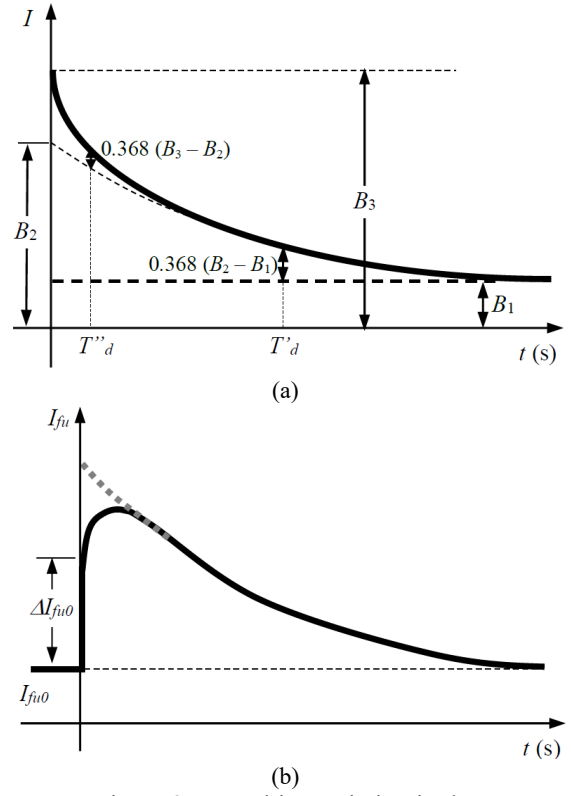


Figure 3. Quantities variation in the sudden short-circuit test.

3.3 Load-rejection Test

The load rejection test is applied to the machine connected to the system, operating as a generator, driven at rated speed, and feeding a purely reactive load. Excitation winding is fed with constant voltage and the machine must be under-excited to avoid overvoltages during the test.

Suddenly, the three-phase terminals of the machine are simultaneously opened, and both armature three-phase voltages and field current are recorded along the transient process. In this test, the terminal voltage steps from zero to a given value, and gradually changes until reaching its final value. The terminal voltage behavior in the voltage recovery test is depicted in Fig. 4a, and the equation that governs the RMS value of the terminal voltage is described in (26).

$$V = V_0 \left\{ 1 - I_0 \left[X_d - (X_d - X'_d) e^{-\frac{t}{T'_{d0}}} - (X'_d - X''_d) e^{-\frac{t}{T''_{d0}}} \right] \right\} \quad (26)$$

Taking into account the absolute values of C_1 , C_2 and C_3 , depicted in Fig. 4a, the synchronous, transient and subtransient reactances are obtained from (27) to (29).

$$X_d = \frac{C_1}{I_0} \quad (27)$$

$$X'_d = \frac{C_2}{I_0} \quad (28)$$

$$X''_d = \frac{C_3}{I_0} \quad (29)$$

Equation (30) describes the behavior of the unidirectional field current related to the initial field current, during the voltage recovery test, as depicted in Fig. 4b.

$$\frac{I_{fu}}{I_{fu0}} = 1 - \left(\frac{X_d - X'_d}{X_d} \right) \left[e^{-\frac{t}{T'_{d0}}} - \left(1 - \frac{T_{1d}}{T''_{d0}} \right) e^{-\frac{t}{T''_{d0}}} \right] \quad (30)$$

Equation (31) is obtained evaluating (30) in the instant zero. Equation (32) comes from the equivalent circuit. Equation (33) results from the solution of (31) and (32) for x equal to x_c .

$$\frac{T_{1d}}{T''_{d0}} = \frac{X_d}{X_d - X'_d} \frac{\Delta I_{fu0}}{I_{fu0}} \quad (31)$$

$$\frac{T_{1d}}{T''_{d0}} = \frac{X''_d - x}{X'_d - x} \quad (32)$$

$$x_c = \left(\frac{T_{1d}}{T''_{d0}} X'_d - X''_d \right) / \left(\frac{T_{1d}}{T''_{d0}} - 1 \right) \quad (33)$$

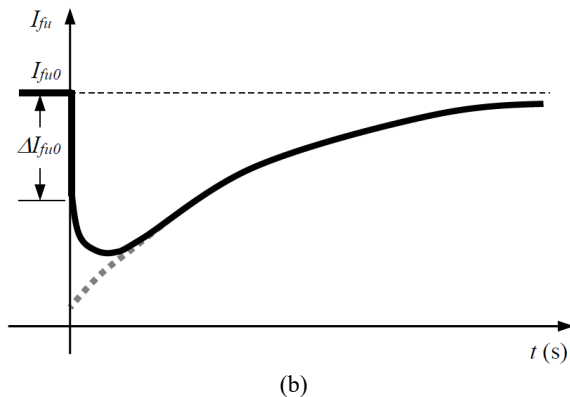
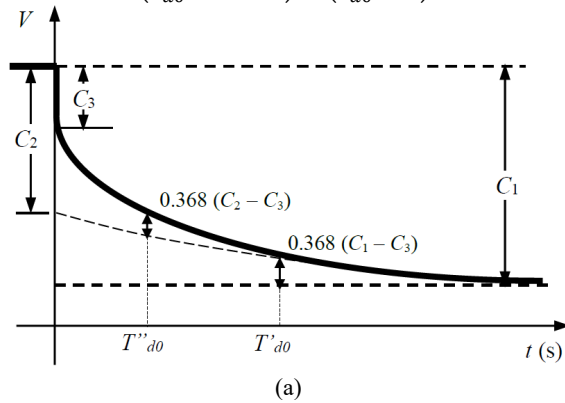


Figure 4. Field current behavior in the load-rejection test.

4 Tests and Simulations

Both three-phase sudden short-circuit and voltage recovery tests have desired and undesired characteristics when compared to each other. For instance, while there is a higher field overcurrent due to the three-

phase short circuit, there is a higher overvoltage in the armature terminals during the short circuit clearing. Both the ampacity of the field winding and the insulation of the armature winding must be consulted with the manufacturer before the application of the test.

Nevertheless, it is interesting to notice the relationship that exists between the field current variations due to the three-phase sudden short-circuit test (SC) and due to the voltage recovery test (VR). This relationship (34) can be obtained from (15) and (23) and can be used to validate obtained results.

$$\frac{(\Delta I_{fu0}/I_{fu0})_{SC}}{(\Delta I_{fu0}/I_{fu0})_{VR}} = \frac{X_d}{X''_d} \quad (34)$$

Tests, simulations, and evaluations were carried out to assess the efficacy of the sequential application of sudden short-circuit and voltage recovery tests. The methods to obtain x_c are also verified with simulation results.

Table 1. Equivalent circuit parameters

X_l	X_{ad}	X_f	X_{ld}	X_{fld}
0.10000	0.90000	0.20000	0.55626	-0.05000

Table 2. Traditional parameters and Canay reactance

X_d	X'_d	X''_d	x_c
0.10000	0.90000	0.20000	0.55626

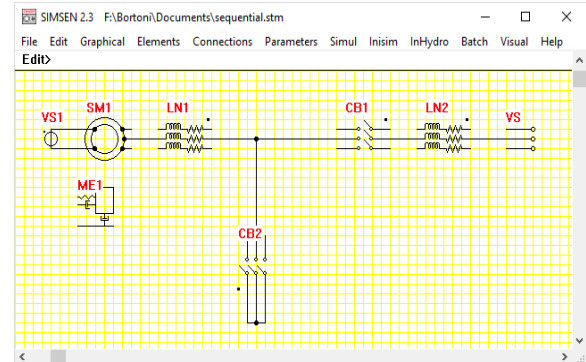


Figure 5. SIMSEN simulation environment.

4.1 Simulation Analysis

The software SIMSEN was employed for the simulation of the circuit depicted in Fig. 5 (Kamwa and Viarouge, 1994). In this circuit, the synchronous machine (SM1) is excited by a fixed voltage source (VS1) and connected to the power system (VS) using two dummy power lines (LN1 and LN2) and a circuit breaker (CB1). The operation of the circuit breaker CB1 allows for load-rejection, while CB2 is used to perform short-circuit and voltage-recovery tests.

The parameters of the d-axis equivalent circuit of the simulated synchronous machine are described in Table 1. Table 2 presents the calculated traditional parameters values.

Figure 6 presents the terminal voltage and field current for the three-phase short-circuit at 5 s and the short-circuit clearing at 15 s. Figures 7a and 7b present details on the field current simulation, for the

sudden short-circuit and for the short-circuit opening, respectively (machine under excited).

In both cases, the initial field current was 0.377 p.u. The field current variation for the simulated three-phase short-circuit test was obtained as 1.1465 p.u., which results in a Canay reactance of 0.0751 p.u. For the voltage recovery test simulation, the initial field current variation was 0.225 p.u., resulting in a Canay reactance of 0.0478 p.u.

It is observed that the Canay reactance resultant from the voltage recovery test was closer to the value of Table 2 than that obtained from the sudden short-circuit test. This difference is explained by the fact that the initial field current variation of the latter is smaller than the actual, due to the influence of the exponential decay in the first peak.

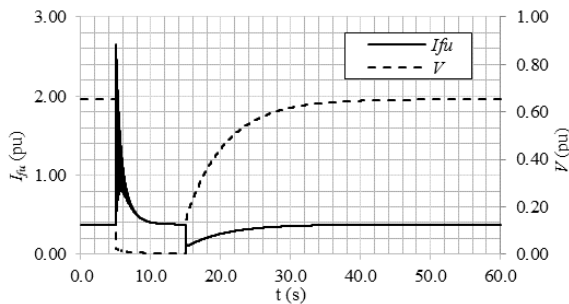


Figure 6. Simulated field current and terminal voltage.

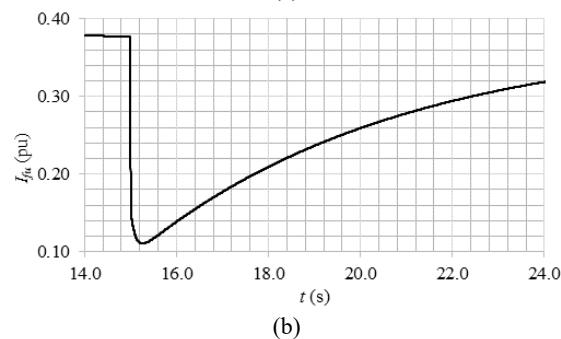
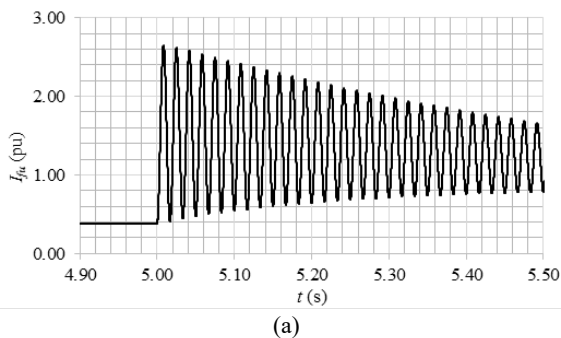


Figure 7. Simulated field current variation.

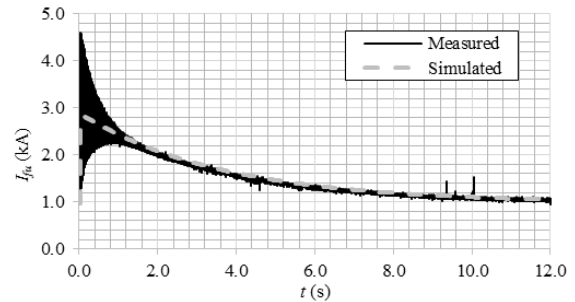
4.2 Evaluation of Field Test Results

In the course of commissioning activities, field circuit current variation was measured along the three-phase short-circuit tests for synchronous generators of 777.8 MVA and of 360 MVA from existent hydropower plants.

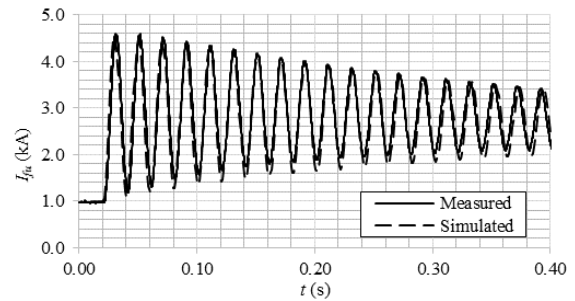
For the 777.8 MVA hydro generator, the per unit values of X_d , X'_d , and X''_d , supplied by the

manufacturer are 0.954, 0.324, and 0.225, respectively. The initial field current was 980 A and the unidirectional initial field current variation was 4600 A. Therefore, the calculations resulted in a Canay reactance of 0.033 p.u. Measurements of the field current and simulations are presented in Fig. 8

The supplied per unit values of X_d , X'_d , and X''_d , for the 360 MVA hydro generator are 1.110, 0.358, and 0.226. The initial field current measured during the test was 450 A and the unidirectional initial field current variation was 2878 A. The calculated Canay reactance was -0.172 p.u. Figure 9 presents the measurement of the field current and its simulations.

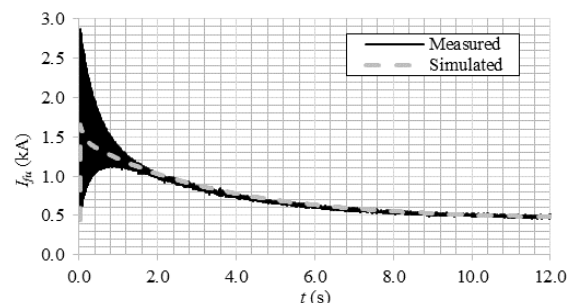


(a)

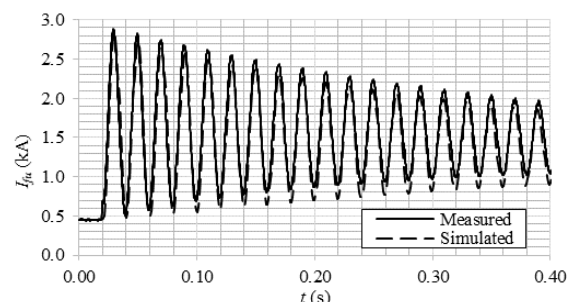


(b)

Figure 8. Field current for the 777.8 MVA generator.



(a)



(b)

Figure 9. Field current for the 360 MVA generator

4.3 Laboratory Application

Three-phase sudden short-circuit and voltage recovery tests were applied to a laboratory synchronous machine. Figure 10 presents the test setup arrangement, while the generator nameplate information is described in Table 3. The machine was driven by a DC motor at its rated speed. Measurements were taken using a Fluke 435 Series II power quality and energy analyzer employing its PowerWave data capture feature.



Figure 10. Laboratory test setup.

Table 3. Laboratory Synchronous Machine Nameplate

Information	Data
Manufacturer	Equacional
Power	2 kVA
Power Factor	0.8
Voltage	133/230/266/460 V
Current	8.7/5.0/4.4/2.5 A
Number of poles	4
Rotational Speed	1800 r/min
Excitation Voltage	220 V
Excitation Current	0.6 A
Insulation Class	F

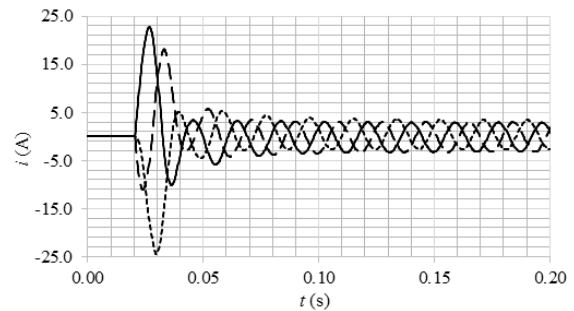
Three phase sudden short-circuit and voltage recovery tests were applied employing the same setup and sequentially. The combined analysis of the armature short-circuit and voltage recovery current lead to per unit values of X_d , X'_d , and X''_d , equals to 1.244, 0.241, and 0.199, respectively.

For the three-phase sudden short-circuit, the initial field circuit current was 0.0975 A and the initial unidirectional field current variation was 0.4563 A, resulting in a Canay reactance of -0.3498 p.u.

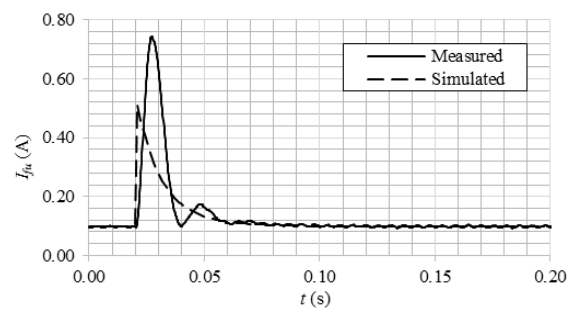
Figure 11 depicts the results from the three-phase sudden short-circuit in terms of the three armature current variation (a) and field circuit current variation measuring and simulation (b).

Considering the voltage recovery test, the initial field current was 0.0978 A and the initial unidirectional field current variation was 0.0733 A, obtaining the value of a Canay reactance of -0.3590 p.u. Figure 16 presents the results obtained with the voltage recovery test from the three-phase short-circuit clearing. Figure 12a shows the behavior of the voltage recovering while Fig. 12b presents the measured field circuit current and unidirectional field current simulation.

It can be observed that there is an excellent agreement between the Canay reactance values obtained in both tests. In addition, the relation between initial field current variations is 6.22 and the relation X_d/X''_d is 6.25, reinforcing the efficacy of the proposal with the sequential application of both tests.

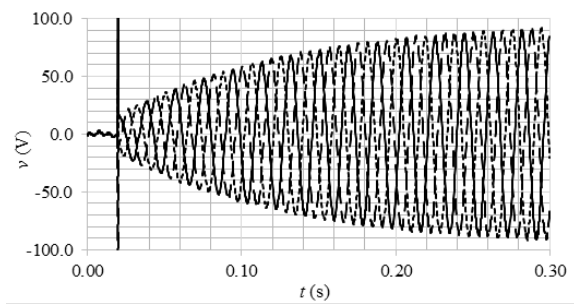


(a)

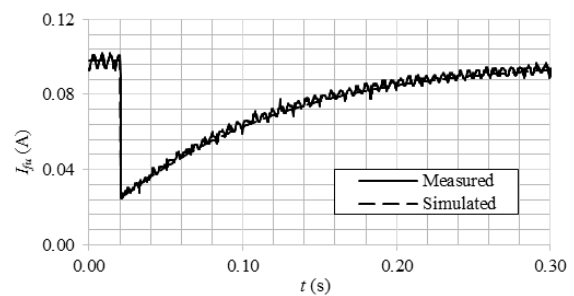


(b)

Figure 11. Armature current and DC component of field current for a three-phase sudden short-circuit test.



(a)



(b)

Figure 12. Armature voltage and field current for the voltage recovery test.

6 Conclusion

While three phase sudden short-circuit and voltage recovery tests have advantages and disadvantages, considering their complementary nature, this paper explored the potentials of their sequential application to model the direct axis of salient pole synchronous generators. The voltage recovery test was treated as a direct axis load rejection instead of using the procedure proposed in the most common machine testing standards.

For sake of the complete modeling, looking for fidelity of the field circuit quantities simulation, the mutual leakage reactance between field and damper windings was considered. Nevertheless, the complete model was converted to the initial one, with equal mutual reactances, using a simple transformation with the obtaining of the Canay reactance. Therefore, the paper also showed methods to obtain the Canay reactance from the aforementioned tests. The proposed methodologies were tested using results from proven simulation software (SIMSEN), from short-circuit applied to two large hydropower generators, and from sequential tests applied to a laboratory machine, reaching a very good agreement between tests and simulations as shown along the paper.

Acknowledgments

The authors appreciate FAPEMIG, CNPq, and INERGE for their continuous support to develop research.

References

- Beordo, L.; Cari, E. P. T.; Landgraf, T. G., and Alberto, L.F.C. (2016). A comparative validation of a synchronous generator by trajectory sensitivity and offline methods. *International Transactions on Electrical Energy Systems*, Vol. 27, No. 2, pp.1-11.
- Bortoni, E. C.; Bernardes, J. V.; Araujo, B. T., and Silva, P. V. V. (2017). Revisiting three-phase sudden short-circuit and voltage recovery tests. *IEEE International Electric Machines and Drives Conference (IEMDC)*. pp. 1-7.
- Bortoni, E. C., and Jardini, J. A. (2002). Identification of Synchronous Machine Parameters Using Load Rejection Test Data. *IEEE Trans. on Energy Conversion*, Vol. 17, No. 2, pp. 242-247.
- Canay, I. M. (1969). Causes of Discrepancies on Calculation of Rotor Quantities and Exact Equivalent Diagrams of the Synchronous Machine. *IEEE Transactions on Power Apparatus and Systems*, Vol. 88, No. 7, pp. 1114-1120.
- IEC 60034-4. (2008). Rotating electrical machines - Part 4: Methods for determining synchronous machine quantities from tests. Edition 3.0. International Electrotechnical Commission, Genève, Switzerland.
- IEEE Std. 1110. (2002). *IEEE Guide for Guide for Synchronous Generator Modeling Practices and Applications in Power System Stability Analyses*. IEEE Power and Energy Society, New York.
- IEEE Std. 115. (2009). *IEEE Guide for Test Procedures for Synchronous Machines Part II- Test Procedures and Parameter Determination for Dynamic Analysis*. IEEE Power and Energy Society, New York.
- IEEE Std. 1812. (2014). *IEEE Trial-Use Guide for Testing Permanent Magnet Machines*. IEEE Power and Energy Society, New York.
- Kamwa, I.; Pilote, M.; Carle, H.; Viarouge, P.; Mpanda-Mabwe, B. and Crappe, M. (1995a). Computer software to automate the graphical analysis of sudden-short-circuit oscillograms of large synchronous machines. *IEEE Transactions on Energy Conversion*, Vol. 10, No. 3, pp. 399-406.
- Kamwa, I.; Pilote, M.; Viarouge, P.; Mpanda-Mabwe, B.; Crappe, M. and Mahfoudi, R. (1995b). Experience with computer-aided graphical analysis of sudden-short-circuit oscillograms of large synchronous machines. *IEEE Transactions on Energy Conversion*, Vol. 10, No. 3, pp. 407-414.
- Kamwa, I. and Viarouge, P. (1994). On Equivalent Circuit Structures for Empirical Modeling of Turbine-Generators. *IEEE Transactions on Energy Conversion*, Vol. 9, No. 3, pp. 579-592.
- Kirtley, J. L. (1994). On turbine-generator rotor equivalent circuits. *IEEE Transactions on Power Systems*, Vol. 9, No. 1, pp. 262-271.
- Martin J. P. and Tindall, C. E. (2000). Computer Analysis of Voltage Recovery and Field Decay Test Responses. *IEEE Transactions on Energy Conversion*, Vol. 15, No. 2, pp. 191-196.
- Mello, F. P., and Ribeiro, J. R. (1977). Derivation of Synchronous Machine Parameters from Tests. *IEEE Trans. on PAS*, Vol. 96, No. 4, pp. 1211-1218.
- SIMSEN. (2017). Simulation Software for Power Networks. Available at: <http://simSEN.epfl.ch/>, accessed 1 June 2017.
- Wamkeue, R.; Jolette, C.; Mabwe, A. B. M.; Kamwa, I. (2011). Cross-Identification of Synchronous Generator Parameters From RTDR Test Time-Domain Analytical Responses. *IEEE Transactions on Energy Conversion*, Vol. 26, No. 3, pp. 776-786.